Chaotic scattering on C_{4v} four-disk billiards: Semiclassical and exact quantum theories

P. Gaspard and D. Alonso
Faculté des Sciences, Université Libre de Bruxelles, Code Postal 231, B-1050 Brussels, Belgium

T. Okuda and K. Nakamura
Department of Applied Physics, Osaka City University, Osaka 558, Japan
(Received 15 April 1994)

We present the semiclassical and exact quantum theories of a point particle bouncing in C_{4v} four-disk billiards, which exhibit chaotic scattering in their classical dynamics. The A_1 sector of the ζ function in the semiclassical trace formula is calculated by using cycle expansions with periodic orbits up to period three in the number of bounces. Its complex poles provide resonances that are in excellent agreement with the exact quantum resonances in a wide range of wave numbers k. Assemblies of resonances lying parallel to the real k axis indicate that the distribution of the imaginary parts of the resonances presents a threshold, and consists of a sequence of small bands below the threshold. The consequences of these resonances on the dynamical behavior of semiconductor mesoscopic devices are briefly discussed.

PACS number(s): 05.45.+b, 03.65.Sq, 03.40.Kf

I. INTRODUCTION

A growing theoretical attention has been given to the chaotic scattering of a point particle by hyperbolic (defocusing) planar billiards. Its classical theory has been well developed in terms of mathematical tools such as the Perron-Frobenius operator, the topological pressure function, as well as other characteristic quantities of chaos [1–4]. In systems with more than two hard disks, it was observed that the unstable orbits which are trapped between the disks constitute a fractal set with zero Lebesgue measure in the three-dimensional phase space. (The three coordinates are, for instance, the positions x, y, and the angle of the velocity vector with respect to the x axis.) Studies on the semiclassical and the full quantum-mechanical counterparts are now constituting a challenging subject in the context of quantum chaos [2–7].

On the other hand, recent progress in the fabrication of nanoscale structures has made it possible to measure the electric conductance, the Hall resistivity, and other quantum transport properties at the so-called crossroad in the $GaAs/Ga_{1-x}Al_xAs$ interfaces [see Fig. 1(a)] [8]. The four corners of the crossroad consist of electron depletion regions which correspond to hard disks in the limit where the potential at the border of the circuit is very steep. While some theoretical studies aim at applying Gutzwiller's semiclassical trace formula to the crossroad problem, their issue (e.g., on conductance) is not in good agreement with the experimental results [8]. This discrepancy would be due to the serious diffraction effect at the leaky regions connected with the straight lead wires. To capture the fluctuation properties truly attributable to chaotic scattering, one should begin to investigate the semiclassical theory of the four-disk system with all its attachments discarded so as to suppress effects of diffraction [see Fig. 1(b)]. The classical study of this system has already been started by Gaspard and Alonso [9].

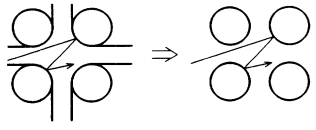

FIG. 1. (a) Crossroad billiard; (b) C_{4v} hard-disk billiard.

In this paper, we shall develop both the semiclassical and the exact quantum theories for a point particle scattered by a model system consisting of our identical hard disks with the C_{4v} symmetry. While the corresponding studies on the C_{3v} three-disk system were made by Gaspard and Rice [2], the change of symmetry and the occurrence of more types of periodic orbits due to the square geometry will address new open questions.

II. EXACT QUANTUM THEORY

Before entering into the semiclassical theory we shall briefly describe the method and results within the framework of the exact quantum theory.

Let us suppose that the four disks $\{d_1,d_2,d_3,d_4\}$ are of unit radius ($a=1$) and are surrounded by a large circle B of radius b which is arbitrary. Denoting the inter-disk distance by R, we assume $2a<R\ll b$. The ratio $\sigma=R/a$ represents the degree of opening: $\sigma\sim 2$ and $\sigma\gg 2$ correspond respectively to a weakly open scatterer with a bulky repeller and to a strongly open scatterer with a filamentary repeller. Moreover, when $\sigma>2.5$, the symbolic dynamics controlling the trapped orbits of the repeller does not demand special pruning rules. The present study will be concerned with the case $\sigma\gg 2.5$ when the corresponding classical dynamics is strongly and fully chaotic.

Consider an incident particle with energy $E=\hbar^2k^2/2m$. The most essential quantity in the scattering problem is the $\underline{S}$ matrix which is introduced in the asymptotic expansion of the wave function in the angular-momentum representation according to

 ©1994 The American Physical Society

$$\Psi_{kl}(\mathbf{r}) \sim \sum_{l'=-\infty}^{+\infty} (2\pi kr)^{-1/2} \left\{ \delta_{ll'} \exp\left[-i\left[kr - l'\frac{\pi}{2} - \frac{\pi}{4} \right] \right] + S_{ll'} \exp\left[i\left[kr - l'\frac{\pi}{2} - \frac{\pi}{4} \right] \right] \right\} \exp(il'\phi) \ . \tag{2.1}$$

At the boundary of $\{d_1, d_2, d_3, d_4\}$, the wave function satisfies

$$\Psi_{kl}(\mathbf{r}_j) = 0 \ , \tag{2.2a}$$

with its normal derivatives expressed as

$$\mathbf{n}_j \cdot \nabla \Psi_{kl}(\mathbf{r}_j) = \sum_{m=-\infty}^{+\infty} A_{ljm} \exp(im\theta_j) \ , \tag{2.2b}$$

where $j = 1, \ldots, 4$.

The unknown quantities $\{S_{ll'}\}$ and $\{A_{ljm}\}$ can be obtained by substituting (2.1), (2.2), and the expression for the free-particle Green function $G(\mathbf{r},\mathbf{r}') = -(i/4)H_0^{(1)}(k|\mathbf{r}-\mathbf{r}'|)$ into Green's theorem which transform bulk integrals into surface integrals. In particular, the $\underline{S}$ matrix is obtained as [2]

$$\underline{S} = \underline{I} - i\underline{C}\,\underline{M}^{-1}\underline{D} \ , \tag{2.3}$$

where $\underline{C}$, $\underline{M}$, and $\underline{D}$ are bi-infinite matrices whose elements contain Bessel functions. This matrix equation is decomposed by using the irreducible representations of the C_{4v} point group. Noting that $A_{l1m} = A_{l2m} = A_{l3m} = A_{l4m}$ with $A_{ljm} = A_{lj-m}$ for the A_1-representation, the components of $\underline{M}^{(A_1)}$ are given as follows:

$$M_{00}^{(A_1)} = \frac{\pi a}{2i}\left[1 + 2\frac{J_0(ka)}{H_0(ka)} H_0(kR) + \frac{J_0(ka)}{H_0(ka)} H_0(\sqrt{2}kR) \right] ,$$

$$M_{0m'}^{(A_1)} = \frac{\pi a}{2i}\left[4\frac{J_0(ka)}{H_{m'}(ka)} H_{-m'}(kR)\cos\left[\frac{\pi m'}{4} \right] + \frac{J_0(ka)}{H_{m'}(ka)} H_{-m'}(\sqrt{2}kR) \right] ,$$

$$M_{m0}^{(A_1)} = \frac{\pi a}{2i}\left[4\frac{J_m(ka)}{H_0(ka)} H_{-m}(kR)\cos\left[\frac{3\pi m}{4} \right] + 2\frac{J_m(ka)}{H_0(ka)} H_m(\sqrt{2}kR)\cos(\pi m) \right] ,$$

$$M_{mm'}^{(A_1)} = \frac{\pi a}{2i}\left\{ 2\delta_{mm'} + 4\frac{J_m(ka)}{H_{m'}(ka)}\left[H_{m-m'}(kR)\cos\frac{(3m-m')\pi}{4} + (-1)^{m'} H_{m+m'}(kR)\cos\frac{(3m+m')\pi}{4} \right] \right.$$
$$\left. + 2\frac{J_m(ka)}{H_{m'}(ka)}\left[H_{m-m'}(\sqrt{2}kR)\cos(m\pi) + (-1)^{m'} H_{m+m'}(\sqrt{2}kR)\cos(m\pi) \right] \right\} , \tag{2.4}$$

where $H_m(z) = H_m^{(1)}(z)$ is the first Hankel function and $m, m' > 0$.

Restricting ourselves to the A_1 representation throughout the present paper, the resonances of the $\underline{S}$ matrix are determined by the zeros of $\det \underline{M}^{(A_1)}(k)$ in the complex plane of the wave number k. We have examined the ranges $-0.4 < \mathrm{Im}k < 0$ with $0 < \mathrm{Re}k < 20$ and $0 < \mathrm{Re}k < 5$ for the ratios $\sigma = 6$ and $\sigma = 12$, respectively. The size of the matrix $\underline{M}^{(A_1)}$ amounts to a dimension of

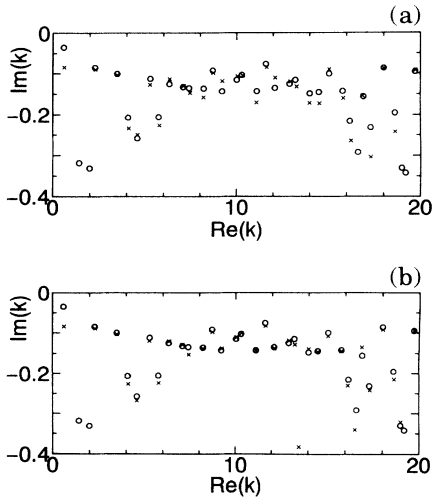

FIG. 2. Exact (○) and semiclassical (×) quantum resonances in the billiard of ratio $\sigma = 6$. The semiclassical results are obtained using (a) 6 orbits with periods 1 and 2; (b) 14 orbits with periods 1, 2, and 3.

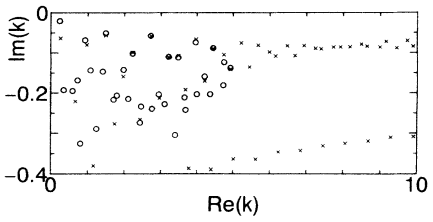

FIG. 3. Same as in Fig. 2 but with $\sigma = 12$. The semiclassical results are obtained using the orbits with periods 1, 2, and 3.

50×50, for us to obtain well-converged values of its (scaled) determinant in the aforementioned complex k domain. The computed quantum resonances are given in Figs. 2 and 3 for $\sigma=6$ and 12 respectively. These figures will be used for comparison with the semiclassical results.

III. SEMICLASSICAL THEORY

According to Balian and Bloch [10], we can define a relative density of state $D(E)$ as the difference between the state densities of the free and of the scattering systems, both confined in the circle B. The relative density $D(E)$ is asymptotically independent of the radius of B and is related to the $\underline{S}$ matrix according to

$$D(E)=\frac{1}{2\pi i}\mathrm{tr}\left[\underline{S}^{\dagger}(E)\frac{d\underline{S}(E)}{dE}\right] . \tag{3.1}$$

Therefore, the density $D(E)$ and the $\underline{S}$ matrix share the same poles. $D(E)$ itself is written as $D(E)=-\pi^{-1}\mathrm{Im}g(E)$ with $g(E)$ being the trace of the difference between the Green functions with and without the four disks.

In the semiclassical limit, $g(E)$ is expressed as a sum over periodic orbits, i.e., by Gutzwiller's trace formula [6]:

$$g(E)=g_0+\sum_p\frac{T_p(E)}{i\hbar}\sum_{r=1}^{\infty}\frac{\exp\left[\frac{i}{\hbar}rS_p(E)+i\pi rL_p\right]}{2\sinh(ru_p/2)} , \tag{3.2}$$

where g_0 is E independent and is given by the difference between the Thomas-Fermi state densities with and without the four disks: $g_0=-4a^2m/(2\hbar^2)$. The prime periodic orbits are labelled by p while the integer r is the number of repetitions of each prime orbit. Denoting by l_p the length of the periodic orbit, $S_p(E)=\oint_p \mathbf{p}\cdot d\mathbf{q}=\hbar k l_p$ and $T_p(E)=dS_p(E)/dE=l_p/v$ are, respectively, the reduced action and the period of p, where $v=\hbar k/m$ is the velocity. (In the classical dynamics of billiards, we mention here that it is often convenient to rescale the velocity to a unit value $v=1$.) L_p is the number of collisions of the orbit p with the disks. The stability exponent u_p is related to the Lyapunov exponent λ_p and the stability eigenvalue Λ_p via $u_p=T_p\lambda_p=\ln|\Lambda_p|$. The latter quantities Λ_p are the eigenvalues of the monodromy matrix $\underline{m}_p$, i.e., of the linearized Poincaré return map in a surface of section transverse to the trajectory. The advantage of the present billiard systems lies in the E independency of Λ_p due to the constancy of the particle velocity, which greatly simplifies the summation in (3.2).

Using the expansion $[2\sinh(x/2)]^{-1}=\sum_{j=0}^{\infty}\exp[-(\frac{1}{2}+j)x]$, the trace function is written in terms of the Ruelle ζ function as [2]

$$g(E)=g_0-\sum_{j=0}^{\infty}\frac{\partial}{\partial E}\ln\zeta_{(1/2)+j}(-ik) , \tag{3.3a}$$

with

$$\zeta_{(1/2)+j}(-ik)=\prod_p\left[1-(-1)^{L_p}\frac{\exp(ikl_p)}{|\Lambda_p|^{1/2}\Lambda_p^j}\right]^{-1} . \tag{3.3b}$$

As a consequence, the complex poles of the Ruelle ζ function yield the resonances of the $\underline{S}$ matrix.

Because of the C_{4v} symmetry of the system, the ζ function can be factorized as $\zeta=\zeta_{A_1}\zeta_{A_2}\zeta_{B_1}\zeta_{B_2}\zeta_E^2$ where the factors correspond to the irreducible representations A_1, A_2, B_1, B_2, and E, the first four of which are one-dimensional while the last one is two-dimensional [11]. This factorization further simplifies the treatment of the product over periodic orbits in (3.3b). We have for instance that $\zeta_{A_1}^{-1}=\prod_p(1-t_p)=1-t_0-t_1-t_2-(t_{01}-t_0t_1+t_{02}-t_0t_2+t_{12}-t_1t_2)-\cdots$, where t_p is given by

$$t_p=(-1)^{L_p}|\Lambda_p|^{-1/2}\exp(ikl_p) , \tag{3.4}$$

if we restrict ourselves to the resonances with the longest lifetimes which are given by the first Ruelle ζ function with $j=0$. In this regard, the A_1 representation we are concerned with in this paper, includes the resonances with the longest lifetimes which are bordering a "gap" void of resonance formed just below the real k axis.

Following the symbolic codings by Cvitanović and Eckhardt [11], the trajectories of the first 14 periodic orbits up to the period 3 in the number of bounces are listed in Table I. The reflection angles φ and the lengths l of these periodic orbits are used to determine the traces of the monodromy matrices according to

TABLE I. Trajectories of the periodic orbits.

period 1	0	12	
	1	1234	
	2	13	
period 2	01	1214	
	02	1243	
	12	12413423	
period 3	001	121232343414	
	002	121343	
	011	121434	
	012	121323	
	021	124324	
	022	124213	
	112	123	
	122	124231342413	

$$\mathrm{tr}\underline{m}=(-1)^n\mathrm{tr}\begin{bmatrix}1+\frac{2l_{n1}\kappa_n}{\cos\varphi_n} & l_{n1}\\ \frac{2\kappa_n}{\cos\varphi_n} & 1\end{bmatrix}\begin{bmatrix}1+\frac{2l_{n-1n}\kappa_{n-1}}{\cos\varphi_{n-1}} & l_{n-1n}\\ \frac{2\kappa_{n-1}}{\cos\varphi_{n-1}} & 1\end{bmatrix}\cdots\begin{bmatrix}1+\frac{2l_{12}\kappa_1}{\cos\varphi_1} & l_{12}\\ \frac{2\kappa_1}{\cos\varphi_1} & 1\end{bmatrix}, \tag{3.5}$$

where $\kappa_n(=1/a$ for all $n)$ is the curvature of the disk where a particle bounces. For the example of the $n=3$ orbit "022" (see Fig. 4), we find $\cos\varphi_1=1$, $\cos\varphi_2=\cos\varphi_3=X$, $l_{12}=Y-a$, $l_{23}=R-2aX$, and $l_{31}=Y-a$, with X and Y satisfying $Y=\{2R^2-2aR[X+(1-X^2)^{1/2}]+a^2\}^{1/2}$ and $2YX(1-X^2)^{1/2}-R+a(1-X^2)^{1/2}=0$. Using $\Lambda_p^2-(\mathrm{tr}\underline{m}_p)\Lambda_p+1=0$, the stability eigenvalues and finally t_p in (3.4) are obtained. It should be noted that the Bunimovich-Sinai curvature formula can also be used to obtained the Lyapunov exponents [2,9].

We have computed ζ_{A_1} for several values of the ratio σ. The zeros of $[\zeta_{A_1}(-ik)]^{-1}$ are obtained by searching for the minima of $|\zeta_{A_1}|^{-1}$ in the complex k plane, whose locations are given in Figs. 2 and 3 in the cases of $\sigma=6$ and 12, respectively. The semiclassical resonances based on 6 orbits with periods 1 and 2 and those based on 14 orbits with periods 1, 2, and 3 are respectively depicted in Figs. 2(a) and 2(b).

In Fig. 2(b), we observe the following.

(i) In a wide window of $0<\mathrm{Re}k<20$ and $-0.4<\mathrm{Im}k<0$, a remarkable agreement is obtained between the locations of the semiclassical and exact quantum-mechanical resonances. While the semiclassical resonances have also been obtained by using orbits up to period 4 [12], no noticeable improvement has been found. Therefore, the semiclassical theory with orbits up to the period 3 is extremely effective in reproducing the quantum resonances. Nevertheless, there remain differences especially for the resonances close to $k=0$. Recent works by two of the authors have shown that these differences can be attributed to diffraction effects and can be taken into account at the next-to-leading semiclassical approximations which include $\hbar$ corrections in the Gutzwiller trace formula (3.2) [13,14].

(ii) The distribution of resonances has a gap below the real k axis. Comparing with the issue for the C_{3v} three-disk system with the same value of σ [2], the gap in the present case is diminished owing to the increase of trapping effect between the four disks (more quantitatively, to the increase of the Hausdorff and information dimensions of the corresponding classical fractal repellers [9]). The semiclassical gap law shows that the resonances obey $\mathrm{Im}k_n<-x_{\mathrm{gap}}$ at large wave numbers $\mathrm{Re}k_n\to\infty$ with the value $x_{\mathrm{gap}}=0.037\,96$ when $\sigma=6$. The resonances close to $k=0$ do not satisfy the inequality because these resonances are strongly affected by diffraction effects explained by the $\hbar$ corrections to the Gutzwiller trace formula [13,14].

(iii) The distribution consists of several quasi periodic structures parallel to the real k axis. In contrast to the C_{3v} three-disk system, the distribution of resonances is here observed to be much more irregular due to the difference between the length scales $\sim R$ and $\sim\sqrt{2}R$ characterizing the square geometry.

Let us proceed with the resonance spectrum of the strongly open scatterer with $\sigma=12$, shown in Fig. 3. The semiclassical resonances are displayed in the window $0<\mathrm{Re}k<10$ and $-0.4<\mathrm{Im}k<0$, but their comparison with their exact quantum counterparts has been done in the limited range $\mathrm{Re}k<5$ because of the too large size of $\underline{M}^{(A_1)}$ required to get converged values of $\det\underline{M}^{(A_1)}$ in the quantal treatment. Nevertheless, the results (i)–(iii) are also valid here.

A careful observation of the periodic structures in Figs. 2(b) and 3 reveals that they are composed of several oscillating strings which lie parallel to the real k axis and merge into narrow bands at high energies to split again at higher energies. To characterize these structures, we shall now analyze dh/dx the density function of the imaginary parts $(x=-\mathrm{Im}k)$ of the semiclassical resonances near the gap, where $h(x)$ is the cumulative distribution function [15]:

$$h(x)=\lim_{(y_2-y_1)\to\infty}\frac{1}{2\pi(y_2-y_1)}[\arg f(x+iy_2)-\arg f(x+iy_1)]\,. \tag{3.6}$$

The function f in (3.6) is the inverse semiclassical ζ function of the A_1 sector: $f(x+iy)=\zeta_{A_1}^{-1}(-ik)$ with $x=-\mathrm{Im}k$ and $y=\mathrm{Re}k$. We choose the ratio $\sigma=12$ where the beating of the oscillating strings is more evident (see Fig. 3). The density dh/dx per unit $\mathrm{Re}k$ is depicted in Fig. 5 for increasing sizes of the interval (y_2-y_1) used in the average (3.6), with $y_1(=8)$ fixed. [Figure 5(d) includes about 150 resonances.] The density consists of a sequence of bands with fine structures near the threshold, which continue to fluctuate as y_2 increases. The formation of bands is caused by the bunching of several oscillating strings parallel to the real k axis. The

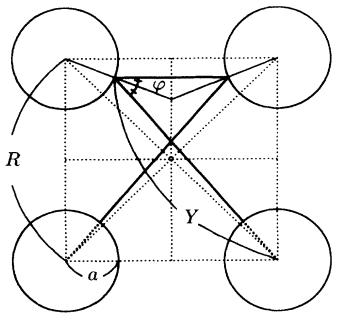

FIG. 4. Period-3 orbit "022."

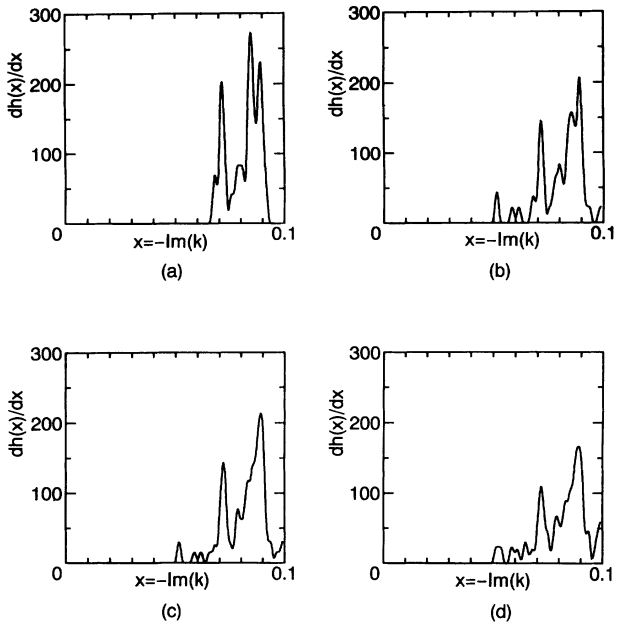

FIG. 5. In the billiard with the ratio $\sigma=12$, density function dh/dx of the imaginary parts of the semiclassical resonances, $x=-\mathrm{Im}k$, obtained with $y_1=8$, and (a) $y_2=20$; (b) $y_2=30$; (c) $y_2=40$; (d) $y_2=50$.

location of a threshold (at $x_{\mathrm{gap}}=0.0509$) in the distribution is extremely stable, ensuring the stability of the resonance gap in the semi-infinite range $\mathrm{Re}k>8$. We should note that, for the separable two-disk billiards [13,16], we have only a single discrete spectrum because of the regular arrangement of resonances parallel to the real k axis at large values of $\mathrm{Re}k$: $dh/dx=\delta(x-x_{\mathrm{gap}})$ with $x_{\mathrm{gap}}=\ln|\Lambda_p|/(2l_p)$. On the other hand, random matrix theories suggest a distribution with the density $dh/dx\propto x^{(\nu/2)-1}\exp(-x/2)$ for ν open channel systems and dimensionless x's. This density is the derivative of the generalized Porter-Thomas cumulative distribution function [17], showing a monotonic growth starting from $\mathrm{Im}k=0$ for $\nu>2$. Because the density of the four-disk scatterer in Fig. 5 shows a behavior which is more complex than in these two special limits, the result of Fig. 5 demonstrates nonuniversality features in the distribution of $x=-\mathrm{Im}k$.

IV. DISCUSSION AND CONCLUSIONS

For C_{4v} four-disk systems, we showed that the exact quantum resonances can be nicely reproduced by the semiclassical theory using the cycle expansion of the Ruelle ζ function with a finite set of periodic orbits up to period 3 in the number of bounces. Small differences remaining between the quantum and the semiclassical resonances may be attributed to higher-order $\hbar$ corrections which can be incorporated in the periodic-orbit quantization as shown recently in Refs. [13,14].

Near the resonance gap, the statistical distribution per unit $\mathrm{Re}k$ of the imaginary parts of the semiclassical resonances turns out to consist of a sequence of bands with small peaks near the threshold. Any finite truncation of the inverse ζ functions should lead to a stable asymptotic distribution $h(x)$ when $\mathrm{Re}k\rightarrow\infty$. However, it seems that the asymptotic distribution is reached only at high values of $\mathrm{Re}k$. On the other hand, there is presently no rigorous result on the existence of this distribution $h(x)$ for the quantum-mechanical system. Besides this question, our results show that the distribution $h(x)$ considerably differs from the prediction of random matrix theories. This difference holds irrespective of the degree of opening of the scatterer and strongly indicates a nonuniversality of the distribution function near the threshold.

The present theory may also be a vehicle for studies on more complicated open systems like the crossroad, where the effect of diffraction should be incorporated. Indeed, the classical repeller of the crossroad billiard differs from the one of the four-disk billiard at the level of the periodic orbit "12" of Table I (see Fig. 1). The periodic orbit "12" is bouncing just at the matching points between the straight lead wires and the circular corners. A recent work [18] has shown that the contribution of such periodic orbits bouncing at discontinuities of the border of the billiard needs to be modified due to special diffraction effects. Such modifications may lead to quantitative differences in the distribution of the resonances between the crossroad and the four-disk billiards but our study indicates that both billiards should share the same qualitative properties. We hope to report on this issue in the future.

To conclude, we mention that the resonances studies in the present paper can provide information on the dynamical behavior of a semiconductor mesoscopic device like the crossroad. The reaction time of the device may be estimated from the size of the aforementioned gap in the distribution of the resonances. Indeed, according to Schrödinger's equation applied to scattering systems, the time evolution of an electronic wave packet is given by a linear superposition of damped exponentials, $\exp(\mathrm{Im}E_n t/\hbar)$, controlled by the imaginary parts of the complex energies of the resonances. In the present system, we showed that the imaginary parts of the wave numbers are bounded by the value of the gap according to $\mathrm{Im}k_n<-x_{\mathrm{gap}}$. Using the relation between energy and wave number, we infer that the probability for the electron to remain in the scatterer decays like $\exp(-t/\tau_{\mathrm{gap}})$. The upper bound on the lifetimes is given by $\tau_{\mathrm{gap}}=1/(2v_F x_{\mathrm{gap}})$ in terms of the semiclassical gap and the Fermi velocity of the electron gas. Since the gap is related to the Lyapunov exponents of the periodic orbits, our analysis shows how the reaction time of the device depend on the geometry of the system:

$$\tau_{\mathrm{gap}}\sim\frac{R}{v_F\ln(R/a)}\ , \tag{4.1}$$

which is valid in the regime $kR, ka\gg 1$ where diffraction effects can be neglected. Therefore, we see that the shortest reaction times are obtained for the smallest values of the corner radius a, assuming a fixed value for the width R of the lead wires. For $\mathrm{GaAs/Ga_{1-x}Al_xAs}$ heterojunctions, the effective mass of the electrons is $m=0.067m_e$

and an electron density of $n_s = 3 \times 10^{11}$ cm^{-2} can be obtained so that the Fermi velocity would then take the value $v_F = \hbar(2\pi n_s)^{1/2}/m = 2.4 \times 10^5$ m/s [8]. For a nanometric circuit of size $R = 100$ nm, the time unit is therefore of $R/v_F = 0.4 \times 10^{-12}$ s so that the lifetimes of the resonances are in the subpicosecond domain [19]. We suggest that the dynamical behavior of such devices could be probed by femtosecond laser experiments.

ACKNOWLEDGMENTS

P.G. thanks the National Fund for Scientific Research (FNRS Belgium) for financial support. D.A. is financially supported by EEC Contract No. ERBCHBICT920097. T.O. and K.N. are grateful to T. Ogawa and Y. Takane for valuable discussions. The Communanté Française de Belgique (Contract No. ARC-93/98-166) is acknowledged for financial support.

[1] D. Ruelle, Phys. Rev. Lett. **56**, 405 (1986); *Thermodynamic Formalism* (Addison-Wesley, Reading, MA, 1978); P. Walters, *An Introduction to Ergodic Theory* (Springer, Berlin, 1981).

[2] P. Gaspard and S. A. Rice, J. Chem. Phys. **90**, 2225 (1989); **90**, 2242 (1989); **90**, 2255 (1989); **91**, E3279 (1989).

[3] P. Gaspard, K. Nakamura, and S. A. Rice, Comments At. Mol. Phys. **25**, 321 (1991); S. A. Rice, P. Gaspard, and K. Nakamura, Adv. Classical Trajectory Methods **1**, 215 (1992).

[4] R. Blümel and U. Smilansky, Physica D **36**, 111 (1989); E. Doron, U. Smilansky, and A. Frenkel, *ibid.* **50**, 367 (1991).

[5] See articles in *Chaos and Quantum Physics,* Proceedings of the Les Houches Summer School, Course LII, 1989, edited by M. J. Giannoni, A. Voros, and J. Zinn-Justin (North-Holland, Amsterdam, 1991).

[6] M. C. Gutzwiller, *Chaos in Classical and Quantum Mechanics* (Springer, New York, 1990).

[7] K. Nakamura, *Quantum Chaos: A New Paradigm of Nonlinear Dynamics* (Cambridge University Press, Cambridge, England, 1993).

[8] C. W. Beenakker and H. van Houten, Phys. Rev. Lett. **63**, 1857 (1989); in *Solid State Physics: Advances in Research and Applications,* edited by H. Ehrenreich and D. Turnbull (Academic, New York, 1991); R. A. Jalabert, H. U. Baranger, and A. D. Stone, Phys. Rev. Lett. **65**, 2442 (1990).

[9] P. Gaspard and D. Alonso, Phys. Rev. A **45**, 8383 (1992).

[10] R. Balian and C. Bloch, Ann. Phys. (N.Y.) **85**, 514 (1974).

[11] P. Cvitanović and B. Eckhardt, Phys. Rev. Lett. **63**, 823 (1989); Nonlinearity **6**, 277 (1993).

[12] P. Gaspard and D. Alonso (unpublished).

[13] P. Gaspard and D. Alonso, Phys. Rev. A **47**, R3468 (1993).

[14] D. Alonso and P. Gaspard, CHAOS **3**, 601 (1993).

[15] B. Jessen and H. Tornehave, Acta Math. **77**, 137 (1945).

[16] W. H. Miller, J. Chem. Phys. **63**, 996 (1975).

[17] C. E. Porter, *Statistical Theories of Spectra: Fluctuations* (Academic, New York, 1965); C. E. Porter and R. G. Thomas, Phys. Rev. **104**, 483 (1956).

[18] D. Alonso and P. Gaspard, J. Phys. A: Math. Gen. **27**, 1599 (1994).

[19] P. Gaspard, in *Quantum Chaos,* Proceedings of the International School of Physics "Enrico Fermi," Course CXIX, Varenna, 1991, edited by G. Casati, I. Guarneri, and U. Smilansky (North-Holland, Amsterdam, 1993), pp. 307–383.